Manuscript #	10-PLBI-RA-6319
Current Revision #	0
Submission Date	2010-02-26 05:22:16
Current Stage	Decision Complete
Title	Automated Identification and Tracking of Focal Adhesions Reveals Phosphorylation of Paxillin at Serine 178 As A Key Regulator of Adhesion Dynamics
Running Title	Automated Analysis Reveals FA Dynamics Regulator
Manuscript Type	Research Article
Special Section	N/A
Corresponding Author	Shawn Gomez (University of North Carolina School of Medicine)
Contributing Authors	Matthew Berginski , Eric Vitriol , Klaus Hahn
Financial Disclosure	This work was supported by NIH grants GM57464 and P01 HL080166 (KMH), startup funds from the UNC School of Medicine (SMG) and the NSF Graduate Research Fellowship Program (MEB). The funders had no role in study design, data collection and analysis, decision to publish, or preparation of the manuscript.
Background Abstract	Focal adhesions (FAs) are macromolecular complexes that provide a linkage between the cell and its external environment. In a motile cell, focal adhesions change size and position to govern cell migration, through the dynamic processes of assembly and disassembly.
Methodology/Principal Findings Abstract	To better understand the dynamic regulation of focal adhesions, we have developed an analysis system for the automated detection, tracking, and data extraction of these structures in living cells. This analysis system was used to quantify the dynamics of fluorescently tagged Paxillin in NIH 3T3 fibroblasts followed via Total Internal Reflection Fluorescence Microscopy (TIR-FM).High content time series included the size, shape, intensity, and position of every adhesion present in a living cell. These properties were followed over time, revealing adhesion lifetime and turnover rates, and segregation of properties into distinct zones. We show how a single point

	mutation in Paxillin at the Jun-kinase phosphorylation site Serine 178 changes FA size, distribution, and rate of assembly.
Conclusions/Significance Abstract	This study provides a detailed, quantitative picture of FA spatiotemporal dynamics as well as a set of tools and methodologies for advancing our understanding of how focal adhesions are dynamically regulated in living cells.
Senior Editor	Liz Williams
Categories	Cell Biology/Cell Adhesion, Cell Biology/Cytoskeleton, Computational Biology/Systems Biology, Molecular Biology/Bioinformatics
Competing Interest	No, there is no competing interest that I should disclose, having read the above statement.
Presubmission Type	No
Decision	View Decision Letter / 2010-04-01
Publication Charges	University of North Carolina at Chapel Hill (Charge: $2,610.00, Accept: $2,610.00)
Ethics Statement	All research involving human participants must have been approved by the authors' institutional review board or equivalent committee(s) and that board must be named by the authors in the manuscript. For research involving human participants, informed consent must have been obtained (or the reason for lack of consent explained, e.g. the data were analyzed anonymously) and all clinical investigation must have been conducted according to the principles expressed in the Declaration of Helsinki. Authors should submit a statement from their ethics committee or institutional review board indicating the approval of the research. We also encourage authors to submit a sample of a patient consent form and may require submission of completed forms on particular occasions. All animal work must have been conducted according to relevant national and international guidelines. In accordance with the recommendations of the Weatherall report, "The use of non-human primates in research," we specifically require authors to include details of animal welfare and steps taken to ameliorate suffering in all work involving non-human primates. The relevant guidelines followed and the committee that approved the study should be identified in the ethics statement. Having read the above, please select a statement below.: No, an ethics statement is not required for this work. Please enter your statement below, and place the same text at the beginning of the Methods section of your manuscript (with the subheading Ethics Statement). Enter "N/A" if you do not require an ethics statement.: N/A
Government Employee	No

Open-Access Agreement	Not Received

Manuscript Items

1. Author Cover Letter File #1 PDF (49KB) Low-res PDF (36KB)
   Source File (PDF) 104KB
2. Article File #1 PDF (116KB)
   Source File (PDF) 133KB
3. Figure 1 - Automating the analysis of focal adhesion images requires a multi-stage pipeline. The first row shows several representative images of fluorescently labeled Paxillin using TIR-FM microscopy. In the second row, a cartoon depiction of the segmented adhesions and the cell edge are shown. Identification of the adhesions in each image allows a set of static morphological and fluorescence intensity-based features to be extracted. The third row shows a single adhesion (highlighted in red) being tracked through the short sample time course. The properties of each adhesion are tracked over time, allowing the large scale dynamics of FA to be determined. PDF (165KB)

   

   Small
   Large Source File (TIF) 469KB
4. Figure 2 - Applying quantitative image processing methods to FA images allows comprehensive characterization of FA properties. (A) One frame from a 200 minute movie of NIH 3T3 cells expressing GFP-Paxillin (the scale bar represents 10μm). (B) The same cell as in (A), with each adhesion outlined in a different color. (C) The entire set of adhesions in an experiment can be visualized by overlaying the adhesions from each microscopy image using a different color for the set of adhesions at each time point. This example includes the adhesions from 198 images. (D) A large range of properties can be extracted from the segmented FA. Five samples are provided. The area histogram was filtered to only include adhesions with areas less than 5μm2. The axial ratio histogram was filtered to only include adhesions with an axial ratio of 8 or less. The longevity histogram includes all adhesions, while the inset only includes adhesions with longevity greater than 20. The histograms include data from 21 cells. PDF (600KB) Low-res PDF (129KB)

   

   Small
   Large Source File (PNG) 792KB
5. Figure 3 - Automated measurement of focal adhesion dynamics. (A) Each of the adhesions in the cells is tracked, allowing the position and properties of single adhesions and populations to be assessed. Here a single adhesion (in green), the surrounding adhesions (in blue) and the cell edge (in red) are followed for 49 minutes. The cell edge is only outlined in the first frame. The scale bar is 10mm. (B) The intensity of EGFP- Paxillin in the tracked adhesion in (A) through time. The green, yellow and red lines are smoothed using the Lowess algorithm and correspond to the assembly, stable and disassembly phases, respectively. (C) The normalized log-linear fit of the Paxillin intensity through time during the assembly phase of the adhesion in part (B). The inset depicts several of the images from which the Paxillin intensity was gathered. (D) The normalized log-linear fit of the Paxillin intensity through time during the disassembly phase of the adhesion in part (B). (E) The assembly and disassembly rates for adhesions whose Paxillin intensity curve fits have R^2 values of 0.9 or greater. The top and bottom lines of the boxes indicate the 3rd and 1st quartiles respectively, while the bold central lines indicate the median values. The whiskers extend up to 1.5 times the interquartile range. PDF (731KB)

Small
Large Source File (TIF) 753KB

6. Figure 4 - Spatial properties of FA positions at birth and death. (A) The majority of adhesions are born within 5μm of the cell edge and the greatest variance in assembly rates are also observed in this 5μm band. (B) The distribution of the distance of death location from the cell edge indicates that adhesion disassembly typically occurs along a broader band from the cell edge as compared to the position at adhesion birth. Also, the variance in disassembly rate is roughly the same regardless of the position at adhesion death. PDF (428KB)

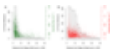

Small
Large Source File (TIF) 378KB

7. Figure 5 - The S178A mutation in Paxillin decreases adhesion size and axial ratio. There were 331558 adhesions in the wild-type and 498644 adhesions in the S178A data sets. The p-values were calculated using a two-tailed t-test. PDF (155KB) Low-res PDF (46KB)

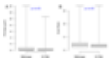

Small
Large Source File (TIF) 77KB

8. Figure 6 - The S178A mutation in Paxillin alters adhesion assembly and disassembly. (A and B) The rate of adhesion assembly and disassembly are significantly decreased by the S178A mutation. The S178A median FA assembly rate is decreased by 42% compared to the wild-type cells, while the median disassembly rate is decreased by 36%. (C and D) The S178A mutation shifts the median adhesion birth location away from the cell edge, but has no effect on the location of cell death. The S178A median adhesion birth position is 31% greater than wild-type median birth position. The median position at adhesion death is decreased by 4% between the S178A and wild-type cells. The blue numbers in each plot are the p-values of the difference in median values between the wild-type and S178A mutants. P-values were calculated using the bootstrapped confidence intervals with 10000 replicates. PDF (358KB) Low-res PDF (93KB)

Small
Large Source File (TIF) 222KB

9. Figure 7 - The lengths of the assembly and disassembly phases in S178A mutant FAs are significantly different from those in the wild-type, while the stability phase lengths are unaffected. The phase length values include all adhesions where the log-linear models fit with a p-value of 0.05 or less. Error bars indicate 99% confidence intervals on the mean phase length as determined through 50,000 bootstrap samples. A double asterisk (**) indicates $p<10^{-5}$ and single asterisk (*) indicates $p<0.05$. Wild-type N Values: Assembly (1068), Stability (465), Disassembly (1392); S178A N Values: Assembly (2106), Stability (870), Disassembly (1802). PDF (224KB) Low-res PDF (60KB)

Small
Large Source File (TIF) 80KB

10. Figure 8 - Summary of results and conceptual model of how the S178A mutant affects the adhesion life cycle. Durations and slopes are shown to scale. PDF (63KB) Low-res PDF (20KB)

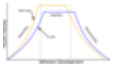

Small
Large Source File (TIF) 226KB

11. Figure S1 - The assembly and disassembly log-linear models fit the Paxillin intensity time courses with high R2 values. The red lines indicate the median length-adjusted R2 values. PDF (403KB) Low-res PDF (107KB)

Small
Large Source File (TIF) 242KB

12. Figure S2 - Flow chart for the tracking software adhesion following algorithm. PDF (121KB) Low-res PDF (37KB)

Small
Large Source File (TIF) 59KB

13. Figure S3 - Changing the adhesion detection threshold does not affect the differences in the assembly rates between S178A mutant and wild-type cells. Each boxplot contains all the adhesions with significant linear fits (linear model p-value below 0.05). The p-values in each boxplot are for the difference in medians between the wild-type and S178A data sets in each boxplot. PDF (472KB) Low-res PDF (117KB)

Small
Large Source File (TIF) 263KB

14. Figure S4 - Changing the adhesion detection threshold does not affect the differences in the disassembly rates between S178A mutant and wild-type cells. Each boxplot contains all the adhesions with significant linear fits (linear model p-value below 0.05). The p-values in each boxplot are for the difference in medians between the wild-type and S178A data sets in each boxplot. PDF (468KB)

Small
Large Source File (TIF) 257KB

15. Figure S5 - Changing the minimum length of the assembly phase does not significantly affect the differences in the assembly rate between the wild-type and S178A mutant cells. Each boxplot contains all the adhesions with significant linear fits (linear model p-value below 0.05). The p-values in each boxplot are for the difference in medians between the wild-type and S178A data sets in each boxplot. PDF (406KB)

Small
Large Source File (TIF) 246KB

16. Figure S6 - Changing the minimum length of the disassembly phase does not significantly affect the differences in the assembly rate between the wild-type and S178A mutant cells. Each boxplot contains all the adhesions with significant linear fits (linear model p-value below 0.05). The 95% confidence intervals on the percent change in the median assembly rate between the wild-type and S178A adhesions overlap in all

minimum length settings. The p-values in each boxplot are for the difference in medians between the wild-type and S178A data sets in each boxplot. PDF (416KB) Low-res PDF (108KB)

Small
Large Source File (TIF) 251KB

17. Figure S7 - Reducing the time between each frame only has mild effects on the assembly and disassembly rates in the wild-type cells. The label 'All' indicates that none of the images were excluded to estimate the rates, while 'Sampled' indicates that every other image from each experiment was discarded. To compensate for the shortened experimental time, the minimum number of points needed to determine an assembly or disassembly rate was reduced to 5 for the sampled data sets. Each boxplot describes the data from all the adhesions with significant linear fits (p-value below 0.05). PDF (334KB) Low-res PDF (88KB)

Small
Large Source File (TIF) 214KB

18. Figure S8 - Reducing the time between each frame only has mild effects on the assembly and disassembly rates in the S178A cells. The label 'All' indicates that none of the images were excluded to estimate the rates, while 'Sampled' indicates that every other image from each experiment was discarded. To compensate for the shortened experimental time, the minimum number of points needed to determine an assembly or disassembly rate was reduced to 5 for the sampled data sets. Each boxplot describes the data from all the adhesions with significant linear fits (p-value below 0.05). PDF (344KB) Low-res PDF (89KB)

Small
Large Source File (TIF) 221KB

19. Figure S9 - Evaluation of the analysis system's ability to extract quantitative properties from simulated stationary focal adhesions. (A) The last frame of the stationary simulation, with each adhesion outlined in a color depending on when in the movie it was born. The adhesions in blue have been detected for the longest time, while those in red and orange have been detected for the shortest amount of time. The simulated adhesions in columns 1-3 are all too faint to be reliably detected for the length of the simulation experiment, while those in column 4 are near the limit of detection. (B) The exponential distribution of adhesion longevity appears similar to that observed in the experimental data. The longevity of all the detected adhesions was correctly identified as 25 minutes. (C and D) The average adhesion intensity (C) and mean adhesion area (D) were correctly identified in the adhesions that were detected for their entire 25 minute lifespan. The red lines in C indicate the true values. PDF (456KB) Low-res PDF (102KB)

Small
Large Source File (TIF) 443KB

20. Figure S10 - Evaluation of the tracking algorithm's ability to follow adhesions of various sizes and speeds. (A) A sample frame from the simulated adhesion motion experiment where the adhesions were moved at 1 pixel per frame. The top row of adhesions of only a single pixel could not be followed. (B) As the movement speed of the simulated adhesions increases, only larger adhesions can be reliably tracked. PDF (188KB) Low-res PDF (43KB)

Small
Large Source File (TIF) 305KB

21. Figure S11 - Evaluation of the rate and phase length detection algorithm using simulated focal adhesion images. (A and C) The predicted median assembly (A) and disassembly (C) rates were extracted correctly by the algorithm. (B and D) The predicted lengths of both the assembly (B) and disassembly (D) were also correctly identified by the algorithm. All the red lines indicate the expected values of the properties in each plot. PDF (471KB) Low-res PDF (125KB)

Small
Large Source File (TIF) 397KB

22. Merged File containing manuscript text and 19 Figure files. PDF (6917KB)

Manuscript Tasks

Decision Summary
Check Status